Which phase is measured in the mesoscopic Aharonov-Bohm interferometer?

A. Aharony[a], O. Entin-Wohlman[a], B. I. Halperin[b] and Y. Imry[c]
[a] *School of Physics and Astronomy, Raymond and Beverly Sackler Faculty of Exact Sciences, Tel Aviv University, Tel Aviv 69978, Israel*
[b] *Department of Physics, Harvard University, Cambridge, MA 02138*
[c] *Department of Condensed Matter Physics, The Weizmann Institute of Science, Rehovot 76100, Israel*
(February 1, 2008)

Mesoscopic solid state Aharonov-Bohm interferometers have been used to measure the "intrinsic" phase, α_{QD}, of the resonant quantum transmission amplitude through a quantum dot (QD). For a two-terminal "closed" interferometer, which conserves the electron current, Onsager's relations require that the measured phase shift β only "jumps" between 0 and π. Additional terminals open the interferometer but then β depends on the details of the opening. Using a theoretical model, we present quantitative criteria (which can be tested experimentally) for β to be equal to the desired α_{QD}: the "lossy" channels near the QD should have both a small transmission and a small reflection.

PACS numbers: 73.63.-b, 03.75.-b, 85.35.Ds

I. INTRODUCTION

Recent advances in the fabrication of nanometer scale electronic devices raised much interest in the quantum mechanics of quantum dots (QDs), which represent artificial atoms with experimentally controllable properties [1,2]. The quantum nature of the QD is reflected by resonant tunneling through it, as measured when the QD is connected via metallic leads to electron reservoirs. The measured conductance G shows peaks whenever the Fermi energy of the electrons crosses a bound state on the QD [3]. Experimentally, the energies of these bound states are varied by controlling the plunger gate voltage on the QD, V. Quantum mechanically, the information on the tunneling is contained in the complex transmission amplitude, $t_{QD} = \sqrt{T_{QD}}e^{i\alpha_{QD}}$. It is thus of great interest to measure both the magnitude T_{QD} and the phase α_{QD}, and study their dependence on V [4]. Although the former can be deduced from measuring G, via the Landauer formula [5], $G = \frac{2e^2}{h}T$, experimental information on the latter has only become accessible since 1995 [6,7], using the Aharonov-Bohm (AB) interferometer [8].

In the AB interferometer, an incoming electronic waveguide is split into two branches, which join again into the outgoing waveguide (see Fig. 1(a)). Aharonov and Bohm [9] predicted that a magnetic flux Φ through the ring would add a difference $\phi = e\Phi/\hbar c$ between the phases of the wave functions in the two branches of the ring, yielding a periodic dependence of the overall transmission T on ϕ. Placing a QD on one of the branches, one expects T also to depend on t_{QD}. Indeed, the experiments found a periodic dependence of $T(\phi)$, and fitted the results to a Fourier expansion of the form

$$T = A + B\cos(\phi + \beta) + C\cos(2\phi + \gamma) + \dots, \qquad (1)$$

with the conventions $B,\ C > 0$.

In a simple two-slit situation, there is no reflection of electrons from either the source or the "screen" which collects them. Therefore, the electron passes through each branch (including the QD) only once, and the total transmission amplitude is equal to the sum of the *amplitudes* in the two branches,

$$t = t_1 e^{i\phi} + t_2. \qquad (2)$$

(Gauge invariance allows one to attach the AB phase ϕ to either branch). Assuming also that $t_1 = |t_1|e^{i\alpha_1} = ct_{QD}$, and that both $c = |c|e^{i\delta}$ and $t_2 = |t_2|e^{i\alpha_2}$ do not depend on V near the QD's resonances, one obtains Eq. (1), with $B = 2|ct_2t_{QD}|$, $C = 0$ (i.e. no higher harmonics) and $\beta = \alpha_{QD} + \delta - \alpha_2$. Below we subtract from α_{QD} and from β their values at large negative V, far away from the resonances, thus removing V-independent quantities like $\delta - \alpha_2$. For the "closed" two-terminal geometry of Fig. 1(a), as used by Yacoby *et al.* [6], the expectation that $\beta = \alpha_{QD}$ (equivalent to the two-slit situation) was clearly not borne out by the measurements: Unitarity (conservation of current) and time reversal symmetry imply the Onsager relations [10,11], which state that $G(\phi) = G(-\phi)$, and therefore β (as well as γ etc.) *must* be equal to zero or π. Indeed, the experimental [6] β "jumps" from 0 to π whenever V crossed a resonance of the QD, and then exhibits an a priori unexpected "phase lapse" back to 0, between every pair of resonances. Later experiments [7] opened the interferometer, using the six-terminal configuration shown schematically in Fig. 1(b); the additional leads allow losses of electronic current, thus breaking unitarity. Indeed, the resulting data gave a gradual increase of β through each resonance, accompanied by a peak in the amplitude B, but maintained the sharp "phase lapse" back to zero between resonances, which were accompanied by zeroes in B. In the present paper we present a theoretical model, aimed to imitate the experimental setups of Fig. 1(a) and (b). Figure 2 shows examples of our model calculations for $A,\ B,\ C$

and β versus V. Qualitatively, these plots look similar to those found experimentally [6,7]. However, as discussed below, the quantitative results for the open interferometers depend on details of the opening.

The above experimental results led to much theoretical discussion. Some of this [12,13] emphasized the nontrivial effects of the ring itself on the measured results, even for the closed case. Other theoretical papers [14–20] *assumed* that the measured β represents the correct α_{QD}, and discussed the possible origins of the observed features, e.g. the "phase lapse" and the similarity between the data at many resonances. However, not much attention was given to the *validity of this assumption*. Since β is equal to 0 or π for the closed interferometer, and deviates from these values for the open one, it is clear that β *must* depend on the details of *how the system was opened*. Indeed, Ref. [21] considered one example of an open interferometer, and showed that the deviation of β from its trivial values (0 and π) increases monotonically with the strength of the coupling to the "lossy" channel. Although different values of this coupling gave *qualitatively* similar $\beta(V)$ curves, which were also similar to the experimental results, the detailed dependence of β on V varied with that strength. As a result, Ref. [21] posed the challenge of finding clear criteria as to when the experimental β is really equal to the intrinsic α_{QD}.

In the present paper we address this challenge [22]. Sec. II presents a simple model for the QD, which contains resonances and "phase lapses". Typical results for the "intrinsic" T_{QD} and α_{QD} are shown in Fig. 3. The latter is also reproduced in Fig. 2 (calculated with the same QD parameters), for comparison with β. We are not aware of any earlier quantitative comparisons of this kind. Sections III and IV then present a simple model for the (closed and open) interferometer, and discusses the optimal way to open the interferometer, so that the "measured" β will be close to the theoretical "intrinsic" α_{QD}. Our exact analytical results confirm the intuitive expectations of Ref. [21]: to have $\beta = \alpha_{QD}$, the electron must cross each branch only once. One necessary condition for this was appreciated qualitatively before [21]: the electron must practically never be reflected from the "forks" where the ring meets the incoming and outgoing terminals, in order to recover the two-slit result (2). In our model, this is achieved by having a very small net transmission after crossing each of the additional "lossy" channels C_ℓ, C_r and C_d in Fig. 1(b). However, we find two additional conditions: first, the transmission through the upper branch, t_1, should have the same phase (up to a V-independent additive constant) as t_{QD}, i.e. α_{QD}. In general, the scattering of the electron from the gates into channels C_ℓ and C_r might cause "rattling" of the electron back and forth through the QD, introducing more phase shifts into t_1. We avoid that by also having a very *small reflection* from the scatterers C_ℓ and C_r. Below we introduce a parameter, J_x, which relates to the tunneling probabilities of the electron from the ring onto the "lossy" channels. As J_x increases, the transmission through the "lossy" scatterers decreases, but the reflection from them increases. Therefore, there is only an *intermediate* range of J_x where $\beta = \alpha_{QD}$ (shown in the lower left box in Fig. 2). The second new condition is that there should be no direct losses from the QD itself; as explained below, these "smear" the "phase lapses". In Sec. V we discuss these results, and propose additional experiments which would check if an open interferometer indeed reproduces the desired "intrinsic" QD information.

II. MODEL FOR THE QD

As in many earlier calculations [12,20,23–25], our analytic calculations are based on the single-electron tight-binding model (which can be viewed as a finite difference version of the continuum case): the system is made of discrete sites $\{i\}$, with nearest neighbor (nn) real tunneling amplitudes $-J_{ij}$ and site energies ϵ_i. All nn distances are set equal to a. The Schrödinger wave equation is thus written as $(E-\epsilon_i)\psi_i = -\sum_j J_{ij}\psi_j$, where the sum is over nn's of i. In each calculation, we have a scattering element connected to two one-dimensional (1D) leads, which have $J_{i,i+1} = J,\ \epsilon_i = 0$. The scattering solution for a wave coming from the left, with wave vector k and energy $E = -2J\cos ka$, is described by $\psi^L_m = e^{ikam} + re^{-ikam}$ on the left, and by $\psi^R_m = te^{ikam}$ on the right. The calculation of the transmission and reflection amplitudes, t and r, then amounts to solving a finite set of linear equations for the wave functions inside the scatterer.

The QD may be described as a single dot, with many discrete energy levels. We model it by a set of smaller dots, each containing a single resonant state, with energy $\{E_R = \epsilon_{QD} = E_R(n),\ n = 1, ..., N\}$. Each such state is connected to its left and right nn's on the leads via bonds with hopping amplitudes $\{-J_L(n),\ -J_R(n),\ n = 1, ..., N\}$. The QD can thus be described by N wave functions ψ_n, obeying $[E-E_R(n)]\psi_n = -J_L(n)\psi^L_0 - J_R(n)\psi^R_0$ (where we choose $\psi^L_0 = 1+r,\ \psi^R_0 = t$). The exact transmission amplitude is easily found to be

$$t_{QD} = \frac{S_{LR}2i\sin ka}{(S_{LL}+e^{-ika})(S_{RR}+e^{-ika}) - |S_{LR}|^2}, \qquad (3)$$

where $S_{XY} = \sum_n J_X(n)J_Y(n)^*/[E-E_R(n)]/J,\ X, Y = L, R$ represent "bare" Green's functions for sites L and R.

In the following, we use equidistant bound state energies, $E_R(n) = V + U(n-1)$. The "gap" U can be viewed as the Hartree energy for an electron added to a QD which already has $n-1$ other electrons [14], thus capturing some aspects of the **Coulomb blockade** behavior of the scattered electron. We study t_{QD} as function of the

energy V, which represents the plunger gate voltage on the QD. Fig. 3 shows typical results for the transmission T_{QD} and for the "intrinsic" phase α_{QD}, where the zero of α_{QD} is set at its ($k-$dependent) value at large negative V. In this figure and below, we choose $ka = \pi/2$, so that $E = 0$ and the resonances of the transmission, where $T_{QD} = 1$, occur exactly when $E_R(n) = E = 0$, i.e. when $V = -U(n-1)$ [26]. Results are not sensitive to k near the band center. We also use the simple symmetric case, $J_L(n) = J_R(n) \equiv J$, and measure all energies in units of J. Interestingly, this model reproduces the apparently observed behavior of α_{QD}: it grows smoothly from 0 to π as E crosses $E_R(n)$, and exhibits a sharp "phase lapse" from π to 0 between neighboring resonances, at points where $T_{QD} = 0$. These latter points, associated with zeroes of S_{LR}, represent Fano-like destructive interference between the states on the QD [28,16,17,27,29].

Many earlier theoretical (e.g. [14]) and experimental (e.g. [7]) papers approximated t by a sum of the single resonance Breit-Wigner-like (BW) expressions [30],

$$t \approx \sum_n \frac{e^{2ika} 2i \sin ka J_L(n) J_R(n)^*}{E - E_R(n) + e^{ika}[|J_L(n)|^2 + |J_R(n)|^2]/J}. \quad (4)$$

Although this form gives an excellent approximation for t_{QD} near each resonance, it completely misses the Fano-like zeroes and the "phase lapses" between resonances. This happens because the approximation moves the zeroes off the real energy axis [27]. As a result, the approximate α_{QD} never reaches 0 or π, and exhibits a smooth decrease from a maximum to a minimum near the correct "phase lapse" values of V. Since our aim here is to check on accurate measurements of the "intrinsic" phase, for a broad range of the parameters, and since the phase lapse has been a topic of much recent discussion [14–20], we prefer to use the exact solutions everywhere. This is particularly important since typically, available experimental data [7] show quite broad resonances, so that the BW approximation is bound to fail between them.

We emphasize again: in spite of the close similarity of our "intrinsic" transmission results with the experiments, the purpose of this paper is not to relate the calculated t_{QD} to the experimental systems. This would require a justification for our choice of the same $J_L(n)$'s and $J_R(n)$'s for all the resonances, which goes beyond the scope of the present paper. Rather, we aim to check when the AB interferometer reproduces the "input" behavior of the QD, by yielding $\beta = \alpha_{QD}$ for all V. If this fails for our simple model then it would surely fail in the more complicated cases, where electron-electron interactions (beyond our simple Hartree approximation) become important [31].

III. MODEL FOR THE CLOSED AB INTERFEROMETER

We next place the above QD on the upper branch of the closed AB interferometer, as shown in Fig. 1(a). We now treat the whole ring as our scatterer: each segment s on the ring is modeled by a 1D tight binding model of M_s sites, with $\epsilon_i = 0$ and $J_{i,i+1} = J_s$ ($s = \ell,\ r,\ d$ for the left and right upper segments and for the lower path, respectively). Taking advantage of gauge invariance, we attach the AB phase factor $e^{i\phi}$ to the hopping amplitude from the right hand "fork" onto its nn on branch r, which we write as $-J_r e^{i\phi}$. Writing the wave functions in segment s as $\psi^s_m = A_s \eta_s^m + B_s \eta_s^{-m}$, with η_s given by $E = -J_s(\eta_s + \eta_s^{-1})$, it is easy to express the total transmission and reflection amplitudes through the interferometer, t and r, in terms of the six amplitudes $\{A_s,\ B_s\}$, and obtain six linear equations whose coefficients also contain $\{S_{XY}\}$. Having solved these equations, one finally finds that the dependence of the total transmission amplitude t on the AB phase ϕ has the general form

$$t = \frac{F + G e^{-i\phi}}{W + Z\cos\phi}, \quad (5)$$

where the complex functions $F,\ G,\ W$ and Z all depend on the other parameters of the QD (including V), the interferometer and the electron wave vector k. It is easy to convince oneself [21] that, apart from an overall multiplicative factor, the numerator represents the two-slit situation of one crossing through each branch of the ring, while the $\cos\phi$ term in the denominator comes from a sum over an infinite geometrical series of additional motions around the ring: clock- and counterclockwise contributions contain factors of $e^{i\phi}$ and $e^{-i\phi}$, multiplying the same complex coefficient. Except for the detailed dependence of the coefficients on V, these facts are model independent. In fact, the form (5) appeared in many earlier model calculations (e.g. [8,23,21,22]). In fact, Eq. (5) implies that the exact form for $T(\phi)$ is

$$T(\phi) = |t|^2 = \frac{A + B\cos(\phi + \beta)}{1 + P\cos\phi + Q\cos^2\phi}. \quad (6)$$

A fit to this equation, instead of the Fourier expansion (1), would be much more accurate (with only five parameters), and would enable an easier comparison of the data with theoretical calculations of $F,\ G,\ W$ and Z.

Using exact integration on $T(\phi)$, the V-dependence of the coefficients in the expansion (1) are presented for the closed interferometer in Fig. 2 (upper left), for the same QD parameters as in Fig. 3. (The figure was produced with $M_\ell = M_r = 6,\ M_d = 12$, but the results for the closed case do not depend on these numbers). For the closed interferometer, time reversal symmetry implies that the ratio F/G in Eq. (5) must be real, and thus T

depends only on $\cos\phi$, in agreement with Onsager's relations. This yields the same jumps of β between zero and π as in Yacoby *et al.*'s experiments [6], coincident with peaks and zeroes of B.

IV. MODEL FOR THE OPEN AB INTERFEROMETER

Pursuing one possible scenario [21], we model the "leaking" from each of the three segments on the ring (imitating C_ℓ, C_r and C_d in the experiment, Fig. 1(b)) by connecting each site on the three ring segments to a 1D lead, which allows only an outgoing current to an absorbing reservoir (Fig. 1(c)). Each such segment is thus replaced by a "comb" of absorbing "teeth".

We start by investigating the properties of a single "comb". The "base" of the "comb" is described by a chain of M tight-binding sites, with $J_{m,m+1} = J_c$ and $\epsilon_m = 0$. Each "tooth" is represented by a 1D tight-binding chain, with $\epsilon_j = 0$. The first bond on the "tooth" has $J_{m,0} = J_x$, while $J_{j,j+1} = J$ for $j \geq 0$. Assuming only outgoing waves on the teeth, with wave functions $t_x e^{ikaj}$ and energy $E = -2J\cos ka$, one can eliminate the "teeth" from the equations. The wave functions on the "base" of the comb are then given by $\psi^c_m = A_c\eta_c^m + B_c\eta_c^{-m}$, where η_c is a solution of the (complex energy) equation $E + J_x^2 e^{ika}/J = -J_c(\eta_c + \eta_c^{-1})$. When this "comb" is treated as our basic scatterer, i.e. connected via $-J_{in}$ and $-J_{out}$ to our "standard" two leads, then the transmission and reflection amplitudes via the "comb" are given (up to unimportant phases) by $t = J_{out}(A_c\eta_c^N + B_c/\eta_c^N)/J$ and $r = J_{in}(A_c\eta_c + B_c/\eta_c)/J - e^{ika}$, and one ends up with two linear equations for A_c and B_c. The results for $T = |t|^2$ and $R = |r|^2$ are shown, for three values of M, in Fig. 4, as functions of $ka \in [0, \pi]$ in the free electron energy band, for $J_x = .7J$ (left), and as functions of J_x, for $ka = \pi/2$ (right). In the figure, $J_c = J_{in} = J_{out} = J$. It is rewarding to observe that both T and R are almost independent of the electron energy E over a broad range near the band center. It is also interesting to note that for these parameters, T decreases with J_x, but R increases with J_x. For fixed J_x, T and R exhibit some even-odd oscillations with M, but basically T decreases with M while R increases towards an almost constant value for $M > 6$. This is understandable: a strong coupling to the "teeth" causes a strong decay of the wave function along the "comb". Thus, for each value of M one can find an intermediate optimal region in which both T and R are small. This region broadens, and has smaller T and R, for larger M.

We next place three such "combs" on the AB interferometer, as in Fig. 1(c), and study the AB transmission T as function of the various parameters. For simplicity, we set the same parameters for all the combs, and vary the coupling strength J_x. Since each "tooth" of the "comb" can be replaced by adding the complex number $J_x^2 e^{ika}/J$ to the energy E in the equations for ψ^s_m on the ring segments, the mathematics is similar of that of the "bare" closed interferometer. The main difference in the results is that now η_c is complex, yielding a decay of the wave function through each comb. This also turns the ratio F/G in Eq. (5) complex, yielding non-trivial values for β. To demonstrate qualitative results, we choose $M_\ell = M_r = 6$, $M_d = 12$, use $J_\ell = J_r = J_d = J_c = J$ and keep $ka = \pi/2$ and the QD parameters $J_L(n) = J_R(n) = J$, $N = 4$, $U = 20J$. The choice for the "comb" parameters ensures that A and B in Eq. (1) are of the same order. Other choices give similar qualitative results. Fig. 2 shows results for A, B, C and β as function of V, for several values of J_x. Clearly, $J_x = .15J$ gives a phase β which is intermediate between the Onsager jumps of the upper left Fig. 2 and the exact intrinsic α_{QD} of Fig. 3. Increasing J_x yields a saturation of β onto α_{QD}, which persists for a broad range between $J_x = .5J$ and $J_x = .9J$. However, larger values of J_x, e.g. $J_x = 1.5J$, cause a deviation of β from α_{QD}, due to the increase of the reflection from each "comb". Interestingly, this deviation is **in the same direction** as for small J_x! The reason for this is clear: as the reflection of each comb increases, the electron "rattles" in and out of the QD. This localizes it on the QD, and reduces the width of the QD resonances. For these large values of J_x, one has $|Z/W| \ll 1$ in Eq. (5). Thus, the two-slit conditions hold, and one has $B \propto |t_1|$ and $\beta = \alpha_1$. We have solved the equations for the transmission through the upper branch only (disconnecting the lower branch altogether), and found that indeed, the coefficient c in $t_1 = ct_{QD}$ is a constant as long as the reflection of the combs is small. However, as J_x increases above about $.9J$, c is no longer a constant. The narrower resonances shown in Fig. 2 (lower right) fully agree with this modified upper branch transmission. In any case, "optimal combs", with small T *and* R, do yield $\beta = \alpha_{QD}$.

So far, we assumed *no* direct losses from the QD itself. It is easy to add such losses, by connecting a "lossy" channel to each resonant state n [21], similar to the "teeth" of our "combs", with a tunneling amplitude J'_x. As before, this introduces a complex addition $J'^2_x e^{ika}$ to $E - E_R(n)$. Fig. 5 shows the results for the same parameters as above, but with $J_x = J'_x = .9J$. Clearly, the new imaginary parts eliminate the Fano-like zero in B, and yield a smooth variation of β near the "intrinsic phase lapses". Although similar to the behavior arising in the BW approximation, the present effects are *real*, due to physical breaking of the unitarity on the QD. It is interesting to note that the data of Ref. [7] show similar (and otherwise unexplained) smooth features. It is however possible that the latter come from finite temperature averaging [27].

V. DISCUSSION

In conclusion, we find that the AB interferometer yields quantitative information on the QD resonances only if the electron crosses each segment on the ring, as well as the QD itself, only once. As stated, this can be rephrased by two criteria: having the two-slit condition – i.e. effectively no reflections back from the "forks" into the ring's branches, and having no "rattling" around the QD – i.e. having little reflection from the "lossy" terminals. A third criterion requires no direct losses from the QD itself.

The two-slit conditions are easy to examine: a small $|Z/W|$ in Eq. (5) implies small amplitudes for all except the first harmonic in Eq. (1), as indeed seen by the decreasing relative values of C for increasing J_x in Fig. 2. This is also easily checked in the analysis of the experimental data [7]. It might be interesting to fit intermediate range data to the exact Eq. (6), instead of using a truncated Fourier series as in Eq. (1).

The second condition, which has not been emphasized in the literature before, is somewhat harder to confirm. One way to check this is to vary J_x experimentally, and look for the value which gives the *largest* width of the resonances. Other ways require disconnecting the lower branch, and studying the conductance through the "lossy" path including the QD and the two "combs". The "combs" are acceptable for our purposes only below a threshold J_x, as long as the conductance peaks remain independent of J_x.

It is worth emphasizing that the experimental data (as reflected in Fig. 2) actually contain more than the AB phase shift β. As stated after Eq. (2), the two-slit condition implies that $B = 2|t_1 t_2|$. Since t_2 is independent of V, this gives $B \propto |t_1|$. Assuming also that the "combs" on the upper branch do not modify the V dependence (i.e. that c is V-independent), we conclude that $T_{QD} = |t_{QD}|^2 = (B/B_{max})^2$, where B_{max} is the maximum of $B(V)$. Indeed, we confirmed that our "data" in Fig. 2 obey this relation in the optimal range of J_x. Moving away from these optimal conditions causes a steeper increase in β, and a related narrower peak in B. Both of these widths should be largest for the optimal conditions. In fact, a third way to ensure a correct measurement of α_{QD} would be to measure T_{QD} directly, from the conductance of the *isolated* QD, and compare it with the normalized B^2 in the interferometer measurement. Obviously, all of the latter experiments require modifications of the mesoscopic circuitry, and may thus not be straightforward to follow.

Although we presented results for only one set of parameters, we emphasize that similar results can be obtained for many other sets. In particular, the results for β and for B/B_{max} do not depend on the parameters of the lower branch. Varying these parameters only adds V-independent factors, and changes the V-dependence of A (which is dominated by the ratio $|t_1/t_2|$). The results are also not sensitive to the sizes M_s of the "combs". However, too broad combs imply too small values of the total transmission through the interferometer (at optimum), giving very small outgoing currents which may be difficult to measure. Thus, although Weidenmüller [22] is right in wishing many terminals, this is not enough. One could also vary other parameters, like J_c, but this might introduce additional resonances, due to the "combs" and not to the QD. Similar undesired comb-related resonances also arise when ka is close to the band edge, but will not arise when one abandons the special 1D treatment of the leads and branches, a situation which is better modeled near the center of the band.

Our analysis also shows that even away from optimum, the *locations* of both the resonances and the Fano-like zeroes (or "phase lapses") are reproduced correctly, independently of the coupling strength J_x. The main purpose of optimizing the interferometer is thus to obtain accurate values of the intrinsic resonance *widths*, which should agree with those found from the direct measurements of the peaks in the isolated QD conductance.

ACKNOWLEDGMENTS

We thank M. Heiblum, Y. Levinson, A. Schiller, H. A. Weidenmüller and A. Yacoby for helpful conversations. This project was carried out in a center of excellence supported by the Israel Science Foundation, with additional support from the Albert Einstein Minerva Center for Theoretical Physics at the Weizmann Institute of Science, from the German Federal Ministry of Education and Research (BMBF) within the Framework of the German-Israeli Project Cooperation (DIP) and from the NSF grant DMR 99-81283.

[1] L. P. Kouwenhoven *et al.*, *Mesoscopic Electron Transport*, NATO Advanced Study Institute, Series E: Applied Science, Vol. **345**, edited by L. L. Sohn, L. P. Kouvwenhoven and G. Schön (Kluwer, Dordrecht, 1997), p. 105.

[2] Y. Imry, *Introduction to Mesoscopic Physics* (Oxford University Press, Oxford 1997; 2nd edition, 2002).

[3] For the purposes of the present paper, it does not matter if the resonant state on the QD involves electron-electron interactions.

[4] Under some analyticity assumptions, α_{QD} can be derived from an integral involving T_{QD} [R. Englman and A. Yahalom, Phys. Rev. B**61**, 2716 (2000)]. However, this requires knowledge of the latter for all values of V.

[5] R. Landauer, Phil. Mag. **21**, 863 (1970).
[6] A. Yacoby, M. Heiblum, D. Mahalu and H. Shtrikman, Phys. Rev. Lett. **74**, 4047 (1995).
[7] R. Schuster *et al.*, Nature **385**, 417 (1997).
[8] Y. Gefen, Y. Imry and M. Ya. Azbel, Phys. Rev. Lett. **52**, 129 (1984).
[9] Y. Aharonov and D. Bohm, Phys. Rev. **115**, 485 (1959).
[10] L. Onsager, Phys. Rev. **38**, 2265 (1931).
[11] M. Büttiker, Phys. Rev. Lett. **57**, 1761 (1986).
[12] J. Wu *et al.*, Phys. Rev. Lett. **80**, 1952 (1998).
[13] K. Kang, Phys. Rev. B**59**, 4608 (1999).
[14] G. Hackenbroich and H. A. Weidenmüller, Europhys. Lett. **38**, 129 (1997).
[15] Y. Oreg and Y. Gefen, Phys. Rev. B**55**, 13726 (1997).
[16] C.-M. Ryu and Y. S. Cho, Phys. Rev. B**58**, 3572 (1998).
[17] H. Xu and W. Sheng, Phys. Rev. B**57**, 11903 (1998).
[18] H.-W. Lee, Phys. Rev. Lett. **82**, 2358 (1999).
[19] P. G. Silvestrov and Y. Imry, Phys. Rev. Lett. **85**, 2565 (2000).
[20] A. Levy Yayati and M. Büttiker, Phys. Rev. B**62**, 7307 (2000).
[21] O. Entin-Wohlman, A. Aharony, Y. Imry, Y. Levinson and A. Schiller, Phys. Rev. Lett. **88**, 166801 (2002); cond-mat/0108064.
[22] Recently, H. A. Weidenmüller [cond-mat/0202197] addressed this question for a QD with a single resonance on a multi-terminal interferometer. He concluded that the two-slit conditions apply in the limit of many terminals, but did not discuss the detailed evolution of the results with the strength of the coupling to the terminals, nor the perturbative effects of the lossy channels in series with the QD.
[23] O. Entin-Wohlman, C. Hartzstein and Y. Imry, Phys. Rev. B**34**, 921 (1986).
[24] J. L. d'Amato, H. M. Pastawski and J. F. Weitz, Phys. Rev. B**39**, 3554 (1989).
[25] D. Kowal, U. Sivan, O. Entin-Wohlman and Y. Imry, Phys. Rev. B**42**, 9009 (1990).
[26] We assume zero temperature, so that E is equal to the Fermi energy. Finite temperature replaces the sharp "phase lapses" by smooth but fast changes [27].
[27] Q. Sun and T. Lin, Euro. Phys. Jour. B**5**, 913 (1998).
[28] U. Fano, Phys. Rev. **124**, 1866 (1961).
[29] O. Entin-Wohlman, A. Aharony, Y. Imry, and Y. Levinson, J. Low Temp. Phys. **126**, 1251 (2002).
[30] G. Breit and E. Wigner, Phys. Rev. **49**, 519 (1936).
[31] Y. Ji, M. Heiblum, D. Sprinzak, D. Mahalu, and H. Shtrikman, Science **290**, 779 (2000).

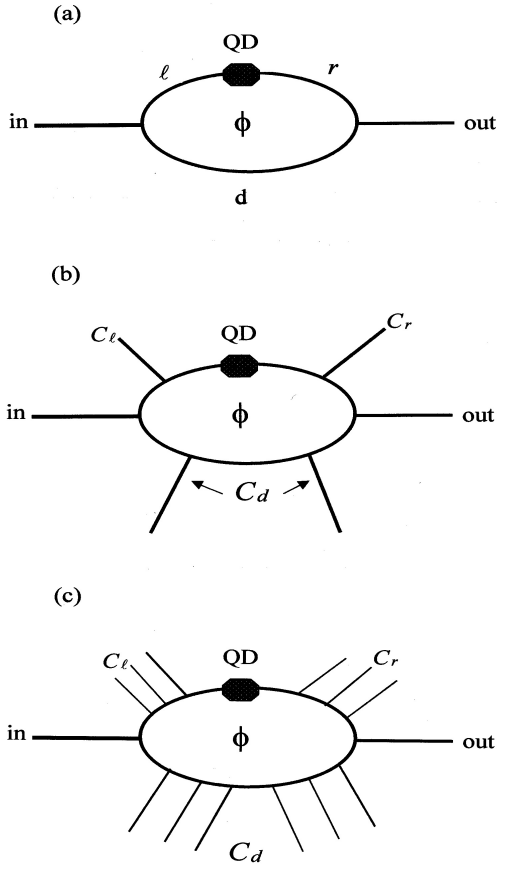

FIG. 1. Model for the AB interferometer: (a) Closed two-terminal case, (b) schematic picture of the six-terminal open interferometer, (c) model for the open interferometer.

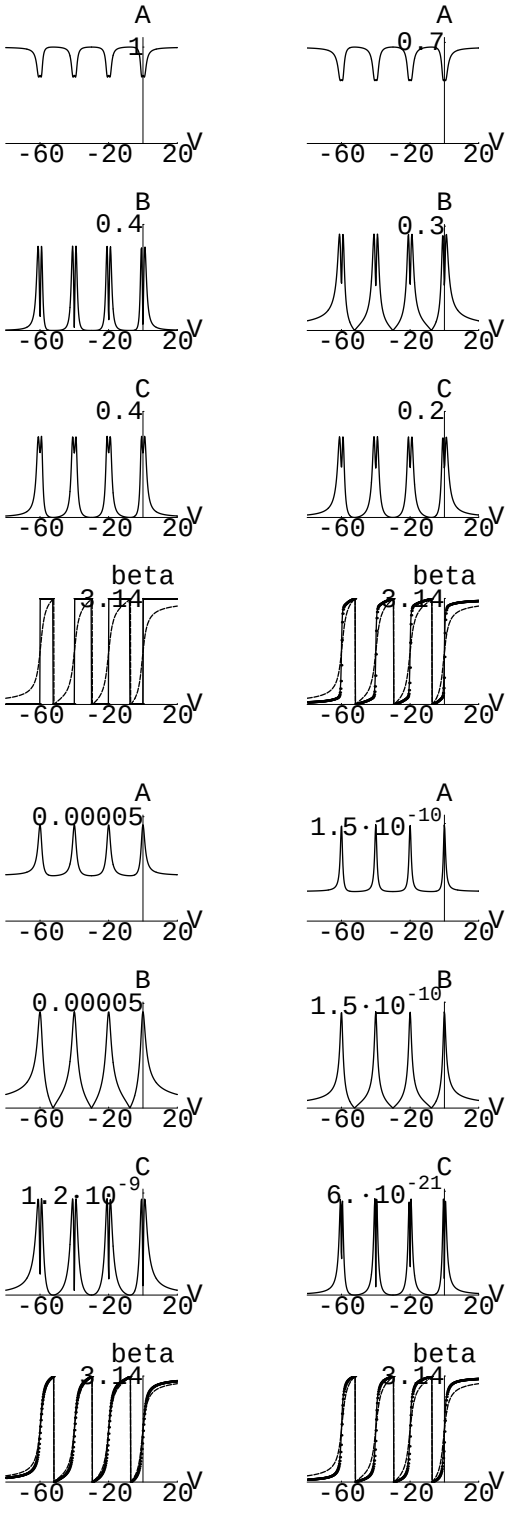

FIG. 2. A, B, C and β for transmission through the closed AB ring (upper left), and for the open interferometer with $J_x = .15J$ (upper right) and $J_x = .9J,\ 1.5J$ (lower left, right). The dashed line shows the exact intrinsic phase α_{QD}.

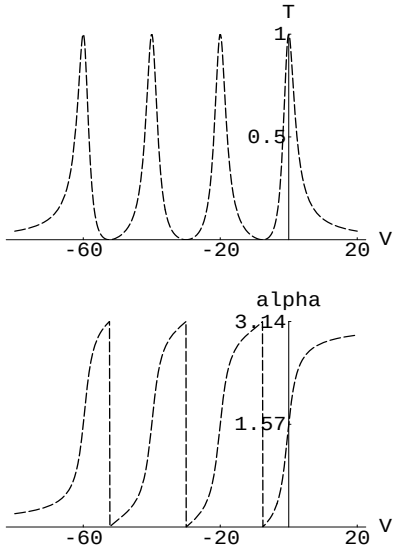

FIG. 3. Transmission T_{QD} and "intrinsic" phase α_{QD} for $N = 4$ states on the QD, with "gap" $U = 20J$, versus the gate voltage V (in units of J).

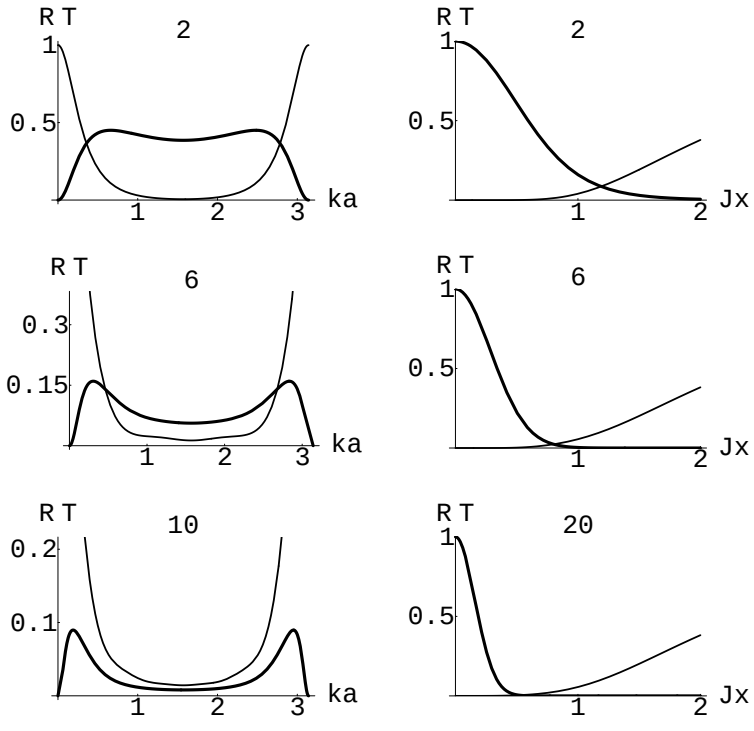

FIG. 4. Transmission (thick line) and reflection (thin line) through a "comb", versus ka at $J_x = .7J$ (left) and versus J_x at $ka = \pi/2$ (right). The number on each frame gives the number of "teeth", M.

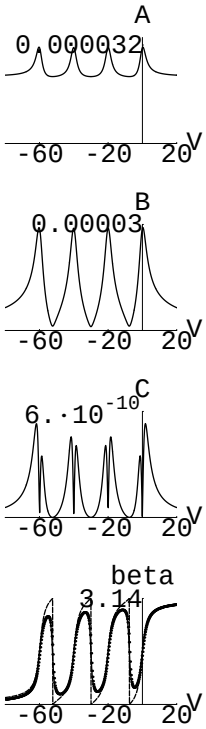

FIG. 5. Same as Fig. 2, but with a "lossy" channel attached to the QD; $J_x = J'_x = .9J$.